Photo-Electro-Oxidation of Alcohols on Titanium Dioxide Thin Film Electrodes

Pablo A. Mandelbaum,[†,‡] Alberto E. Regazzoni,*[,§,||] Miguel A. Blesa,[§,⊥] and Sara A. Bilmes*[,†,#]

INQUIMAE-DQIAQF, Facultad de Ciencias Exactas y Naturales, Universidad de Buenos Aires, Ciudad Universitaria, Pabellón II, 1428 Buenos Aires, Argentina, and Unidad de Actividad Química, Comisión Nacional de Energía Atómica, Avenida del Libertador 8250, 1429 Buenos Aires, Argentina

Received: December 29, 1998; In Final Form: April 19, 1999

The photo-electro-oxidation on titanium dioxide film electrodes of methanol, 2-propanol, and *tert*-butyl alcohol has been studied by measuring the transient photocurrents observed during the early stages of illumination. Transients and steady-state photocurrents, measured at different applied potentials and methanol concentrations, were compared with model predictions. The numerical solution of the differential equations corresponding to methanol photo-electro-oxidation, as well as the advanced experimental evidence, supports the hypothesis that surface hole trapping as $-OH^{\bullet}$ mediates the charge transfer to methanol. Formation of $-OH^{\bullet}$ accounts for the high initial photocurrents, its rapid decay being due to recombination. The rate of oxidation of methanol is then determined by the rate of reaction between $-OH^{\bullet}$ and CH_3OH located in the interfacial region. The oxidation of $^{\bullet}CH_2OH$ to CH_2O, through the injection of an electron into the conduction band (current doubling), gives rise to an increase in photocurrent; steady state values are later attained. As a consequence, a minimum transient is observed. The minimum is marginally observable in *tert*-butyl alcohol solutions, in line with the properties of the respective radicals.

Introduction

Titanium dioxide is a very active and widely used photocatalyst, and its ability to enact the oxidation of many organic compounds, including microorganisms, the conversion of inorganic anions, and the removal of metals by photochemical reduction has been amply demonstrated. Indeed, TiO_2 photocatalysis constitutes the basis of an advanced oxidation process that shows promise for the complete mineralization of organic contaminants.[1−9] One design question relates to the performance of slurry photoreactors as compared to that of fixed-bed ones. However, if the substrate is a conducting one, the net efficiency can be improved by the application of a suitable external bias potential;[10−14] viz., the electron−hole recombination is minimized as photogenerated electrons are driven away from the catalyst/electrolyte interface. Also, complete oxidation can be achieved without the requirement of added electron scavengers.

From the fundamental point of view, there are still open questions concerning the reaction mechanism. Even for simple molecules, the reaction mechanism is complex and depends on several factors, including the nature of all organic and inorganic species present in solution, their concentrations, and solution pH. Certainly, the reactions that take place at the TiO_2/electrolyte interface should be heavily influenced by the characteristics of ionic and molecular adsorption. Interfacial hole transfer to surface hydroxide ions is well-documented,[15−20] but its participation in the mechanism of oxidation of organic molecules is yet unclear. Different cases may be foreseen, depending on the surface−acceptor distance, which, in turn, is related to the nature of the adsorption and to the acceptor affinity for holes. Methanol, for example, is a well-known $OH^{\bullet}$ scavenger: the homogeneous bimolecular rate constant is 9.2×10^8 mol dm^{-3} s^{-1}.[21] Other aliphatic alcohols behave similarly and are known to oxidize readily on illuminated titanium dioxide surfaces.[22−27]

An important point is the role played by the adsorption. A recent work on the photocatalytic dehydrogenation of alcohols on TiO_2 rutile single crystals under ultrahigh vacuum has reported that dissociative chemisorption is a necessary requisite to achieve oxidation.[28] The alkoxy species coordinate to surface Ti^{4+} sites, taking up the dangling bonds produced by bridging-oxygen vacancies. In concordance, the photocatalytic activity increases with the density of oxygen vacancies arising from surface or subsurface defects. In aqueous media, on the other hand, chemisorption of short chain aliphatic alcohols on TiO_2 should be negligible. In fact, on the grounds established by the surface complexation approach,[29−31] no special affinity can be envisaged. The formation of surface alkoxy species of the type $\equiv$Ti−OR competes unfavorably with dissociative water chemisorption, a fact noted by Bohem several years ago.[32]

Electrochemical techniques provide a powerful method for the study of charge-transfer processes at semiconductor/electrolyte interfaces. They allow determination of parameters such as the steady-state interfacial potential,[3] the oxidation length (i.e., the number of oxidation steps triggered by each single hole transfer),[33] and the faradaic efficiency.[34] Moreover, potentiostatic transients obtained upon shining light provide much more detailed information about the dynamics of the interfacial charge-transfer reactions.[35]

In this work we report the photoelectrochemical response of TiO_2 film electrodes immersed in acidic aqueous solutions of methanol, 2-propanol, and *tert*-butyl alcohol, and propose a mechanism in which the oxidation of the alcohols is mediated by $-OH^{\bullet}$ radicals formed upon hole capture by surface $-OH$ groups; the mechanism also includes charge recombination and

* Corresponding authors.
† Universidad de Buenos Aires.
‡ E-mail: pmandel@q3.fcen.uba.ar.
§ Comisión Nacional de Energía Atomica.
|| E-mail: regazzon@cnea.edu.ar.
⊥ E-mail: miblesa@cnea.edu.ar.
E-mail: sarabil@q3.fcen.uba.ar.

10.1021/jp984812h CCC: $18.00
Published on Web 06/11/1999

electron injection into the conduction band by intermediate alkoxy radicals and takes into account the low adsorption affinity of the alcohols. The proposed mechanism accounts for the enhancements of the steady-state photocurrents, for the potentiostatic transients observed before photocurrents attain their steady-state values, and for the negligible steady-state concentrations of $-OH^{\bullet}$ radicals.

Experimental Section

TiO_2 Film Electrodes Preparation. Titanium dioxide films were prepared by the sol−gel route. Sols prepared by hydrolysis of Ti(IV) butoxide at pH < 1 were dialyzed against water up to pH 3.4. The resulting gel was spin coated onto conducting indium−tin oxide (ITO) glass and heated at 90 °C for 5 min. This procedure was repeated six times; after the sixth deposit, the assembly was sintered at 400 °C in air during 6 h. The average thickness of the films was (300 ± 50) nm, as determined by profilometry and by atomic force microscopy (AFM). The mean particle diameter determined by AFM was 200 nm. X-ray diffraction patterns indicate that the films have low crystallinity, the main peaks corresponding to anatase.

The electrodes were built by welding with indium a copper wire to the ITO. Contacts and edges were masked with galvanoplastic lacquer. The geometrical electrode surface area was 0.6 cm^2.

Photoelectrochemical Measurements. Measurements were carried out in a conventional 20 mL three-electrode cell with a quartz window. A saturated calomel electrode (SCE) and a platinum gauze were used as reference and counter electrodes. A homemade potentiostat with automatic data acquisition was employed for controlling the potential of the working electrode and simultaneous current measurements. The light of a 150 W Xe lamp was focused on the TiO_2 film electrode surface. Undesirable heating was avoided using a 15 cm optical length $CuSO_4$ filter at the lamp output for infrared and near-infrared radiation absorption. Direct photolysis of dissolved alcohol was prevented using a 320 nm cutoff filter. The photon flux incident on the electrode was 6.2×10^{-7} einstein s^{-1}, as determined by ferrioxalate actinometry.

All photoelectrochemical experiments were carried out at room temperature (23 ± 1 °C) in N_2-saturated 0.2 M $NaClO_4$ at pH 3, in the presence of adequate concentrations of methanol, 2-propanol, or *tert*-butyl alcohol. Prior to each experiment, several potential cycles were performed in the dark at 0.2 V s^{-1} between − 0.7 and 0.3 V, to achieve reproducible current−potential profiles. These profiles are independent of the presence of the alcohol. Photocurrent transients at a fixed potential were measured after the potential was held at a prefixed value, and a shutter was triggered with synchronic measurement of photocurrent.

Unless otherwise specified, all reagents were analytical grade or better. High purity Milli-Q water was used.

Results

Figure 1a shows that the steady-state photocurrent ($I_{ph,ss}$) vs. potential (E) profile in N_2-saturated base electrolyte at pH 3 is modified by the presence of methanol; as observed also for 2-propanol and *tert*-butyl alcohol, the photocurrent increases at any potential above an onset value of ca. − 0.6 V (Figure 1b). The steady-state photocurrent for 2-propanol and *tert*-butyl alcohol slightly depends on mass transport, and this fact is not observed for methanol. However, with vigorous stirring at the same alcohol concentration, the enhancement of the photocurrent

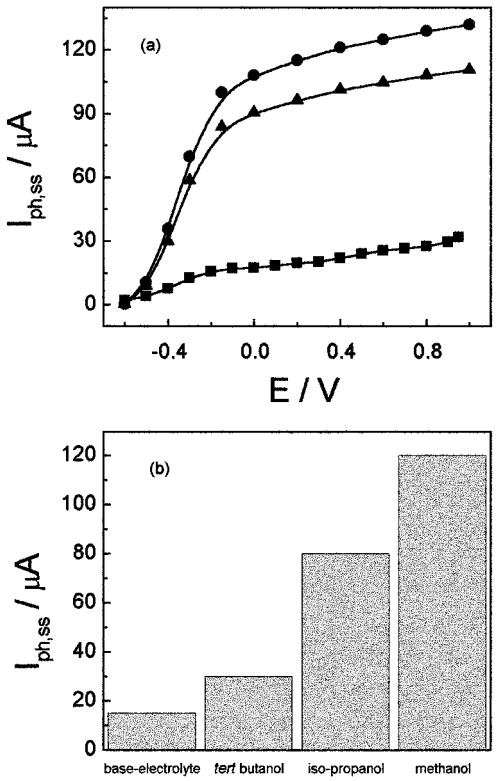

Figure 1. (a) Influence of methanol concentration on the steady-state photocurrent vs potential profiles in 0.2 M $NaClO_4$ at pH = 3: (●) 0.16 M methanol, (▲) 0.08 M methanol, (■) base electrolyte. (b) Dependence of the steady-state photocurrent on alcohol nature; the alcohol concentration is 0.16 M in all cases.

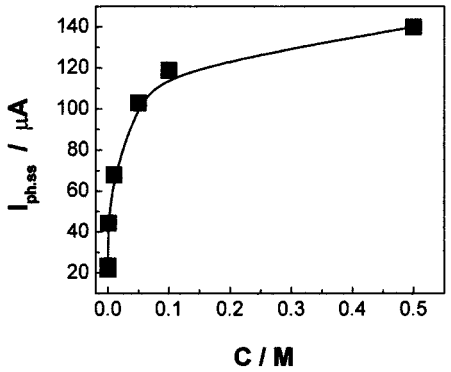

Figure 2. Dependence of the steady-state photocurrent at 0.6 V on methanol concentration in 0.2 M $NaClO_4$ at pH = 3.

at a fixed applied potential decreases in the sequence methanol > 2-propanol > *tert*-butyl alcohol. The dependence of $I_{ph,ss}$ on methanol concentration at 0.6 V is shown in Figure 2.

Upon illumination, at a fixed applied potential, photocurrent transients are observed (Figure 3). In all cases, the photocurrent rises immediately (in a time scale that is below our detection limit) and later decays in a way that depends on solution composition. In the base electrolyte, I_{ph} decreases monotonically until a stationary value is reached. In the presence of the alcohols, photocurrents fall down to a minimum and later increase up to steady-state values. The depth of the minima decreases in the sequence methanol > 2-propanol > *tert*-butyl alcohol, the same trend found for the photocurrent enhancements. The photocurrent decay observed for 2-propanol and *tert*-butyl alcohol for times higher than ca. 20 s is affected by stirring, whereas the depth and location of the minimum remains unaltered. The depth of the minima is potential dependent. As

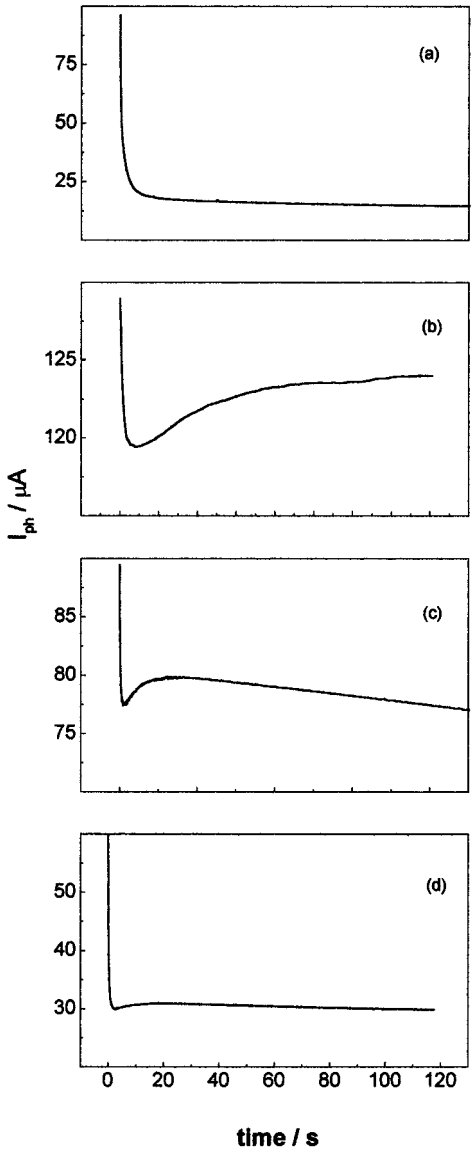

Figure 3. Photocurrent transients in base electrolyte (a), methanol (b), 2-propanol (c), and *tert*-butyl alcohol (d) at 0.6 V in 0.2 M $NaClO_4$ at pH = 3; the alcohol concentration is 0.16 M in all cases.

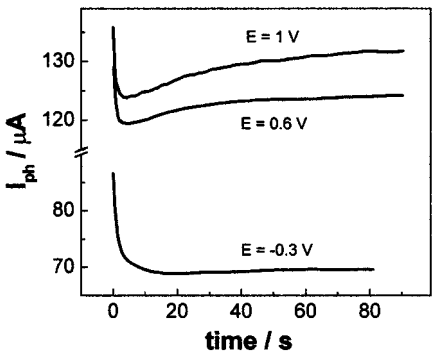

Figure 4. Photocurrent transients for methanol photo-electro-oxidation at different potentials for a 0.16 M methanol solution in 0.2 M $NaClO_4$ at pH = 3.

shown in Figure 4, for methanol, it increases as the applied potential is made more positive.

Figure 5 shows the cathodic sweep (in the dark) after the irradiation, for 3 min at 0.6 V, of the TiO_2 film electrode immersed in the base electrolyte (curve a) and in 0.16 M methanol (curve b). The peak at − 0.4 V and the shoulder at

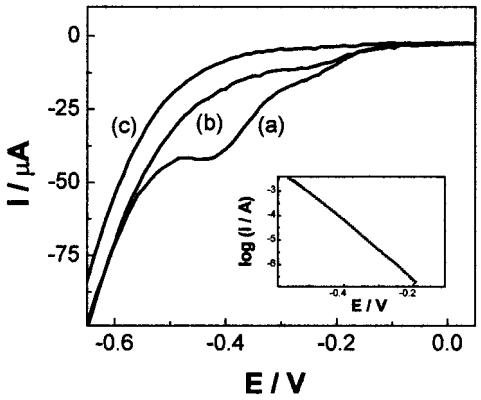

Figure 5. Dark cathodic sweeps after 3 min irradiation at 0.6 V: base electrolyte (a), 0.16 M methanol (b), subsequent sweeps (c). Inset: curve (c) plotted in logarithmic scale.

−0.25 V observed in curve (a) reveal the reduction of long-lived oxidized surface species formed during the irradiation in base electrolyte; these oxidized species are not detected in the subsequent dark sweep in the anodic direction (curve c). In the presence of methanol, the oxidized species do not survive long enough to be seen in the cathodic sweep (curve b).

The plot of ln I vs E (see inset in Figure 5), derived from curve (c), is typical for nonideal Schottky junctions; the factor $m = (e/kT)/\{d(\ln I)/dE\} = 2.8 \pm 0.2$ indicates that ca. 35% of the applied potential drops within the semiconductor space charge layer.

Discussion

Any kinetic model describing the photoelectrooxidation of the studied short chain aliphatic alcohols should be able to account for (i) the dependence of the steady-state photocurrent on alcohol nature and concentration; (ii) the dependence of the photocurrent transient minima on applied potential; (iii) the absence of long-lived oxidized species upon illumination in alcohol solutions; and (iv) the decrease in depth of the photocurrent transient minima when methanol is substituted by ramified alcohols. In principle, all these observations can be explained on the basis of the following set of kinetic equations:

$$TiO_2 + h\nu \rightarrow h_{vb} + e_{cb} \quad \upsilon_1 = k_1 \tag{1}$$

$$-OH + h_{vb} \rightarrow -OH^{\bullet} \quad \upsilon_2 = k_2(OH)(h_{vb}) \tag{2}$$

$$-OH^{\bullet} + e_{cb} \rightarrow -OH \quad \upsilon_3 = k_3(OH^{\bullet})(e_{cb}) \tag{3}$$

$$-OH^{\bullet} + R \rightarrow -OH + R^{\bullet} \quad \upsilon_4 = k_4(R)(OH^{\bullet}) \tag{4}$$

$$R + h_{vb} \rightarrow R^{\bullet} \quad \upsilon_5 = k_5(R)(h_{vb}) \tag{5}$$

$$R^{\bullet} \rightarrow R^{+} + e_{cb} \quad \upsilon_6 = k_6(R^{\bullet}) \tag{6}$$

$$R^{\bullet} + e_{cb} \rightarrow R \quad \upsilon_7 = k_7(R^{\bullet})(e_{cb}) \tag{7}$$

Where all velocities, υ, are given in $cm^{-2}\ s^{-1}$, and the species in parentheses represent the surface concentration of the species in cm^{-2}. Since in aqueous media the alcohols do not chemisorbe,[29,32] they are dissolved in a thin interfacial layer vicinal to the surface, and their surface concentration values, (R), relate to the actual volume concentration throughout the finite thickness of the reaction volume within which they are able to participate in the interfacial charge-transfer reactions. The above overall mechanism further implies that photocurrents are not limited by mass transfer, as is the case for methanol.

Step 1 corresponds to the formation of an electron−hole pair upon irradiation. The fraction of e^-−h^+ pairs recombined during the transit of the carriers to the ITO/TiO_2 and the TiO_2/electrolyte interfaces is taken into account in the value of k_1; note that bulk electron−hole recombination takes place in a time scale that is much shorter than those of the interfacial reactions studied here.[36] Step 3 describes the recombination of e_{cb} with trapped holes formed in step 2; k_3 must be potential dependent, as the applied anodic voltage leads to a larger electron drift to the back contact. Steps 4 and 5 represent two ways in which the radicals, R•, can be produced, either by reaction with trapped holes (eq 4) or by direct hole transfer (eq 5). Step 6 represents electron injection into the conduction band by the radicals, a characteristic of several organic species.[37−39] R^+ denotes the intermediate products that are formed in step 6, and in the case of methanol they can be identified as formaldehyde.[39,40] Their likely oxidation is not included in the kinetic scheme depicted by eqs 1−7 because the conversion degree was always insignificant; indeed, in all cases the circulated charge was negligible as compared to the amount of available alcohol. Step 7 describes the charge recombination involving R• radicals and e_{cb}; k_7 must be also potential dependent. The R• species from methanol and 2-propanol are α-hydroxyl radicals and β-hydroxyl radical for *tert*-butyl alcohol.

Equations 1−7 lead to the following set of differential equations:

$$d(h_{vb})/dt = \upsilon_1 - \upsilon_2 - \upsilon_5 \quad (8)$$

$$d(e_{cb})/dt = -I_{ph}/(FA) + \upsilon_1 - \upsilon_3 + \upsilon_6 - \upsilon_7 \quad (9)$$

$$d(R^\bullet)/dt = \upsilon_4 + \upsilon_5 - \upsilon_6 - \upsilon_7 \quad (10)$$

$$d(OH^\bullet)/dt = \upsilon_2 - \upsilon_3 - \upsilon_4 \quad (11)$$

In eq 9, F is the Faraday constant and A is the electrode area. Assuming that electroneutrality is instantaneously attained (i.e., equal hole and electron fluxes), the time dependence of I_{ph} is given by

$$(I_{ph}/FA) = \upsilon_2 + \upsilon_5 - \upsilon_3 + \upsilon_6 - \upsilon_7 \quad (12)$$

This set of differential equations was solved numerically, the four independent variables, (h_{vb}), (e_{cb}), ($OH^\bullet$), ($R^\bullet$) being reduced to three by eq 12 and the surface mass balance; since no change in surface area by photocorrosion or any other process could be detected, the total number of surface hydroxyls, $(OH)_0$, is assumed to be constant. $(OH)_0$ and the set of rate constants were derived from the fitting of the data. A fit was considered satisfactory when the difference between the calculated and the experimental total circulated charge fell below 0.1 μC, except for the most extreme potentials, for which an error of 7 μC was considered acceptable.

To assess the relative contributions of steps 4 and 5 to the overall photo-electro-oxidation of the alcohols, two limiting cases were analyzed. In the first one, mechanism A, surface −OH groups do not trap holes (i.e., $\upsilon_2 = 0$), which are directly transferred to the alcohol molecules dissolved in the interfacial layer. In the second, mechanism B, the holes are transferred to the alcohol molecules via $-OH^\bullet$ only (i.e., $\upsilon_5 = 0$). The following discussion is focused on the behavior of methanol, which is independent of mass transport; comparison with the other alcohols will be made whenever relevant. Experimental and calculated transients are compared in Figure 6 for both reaction pathways. The fitting of mechanism B is better, although that of mechanism A is also acceptable. These mechanisms, however,

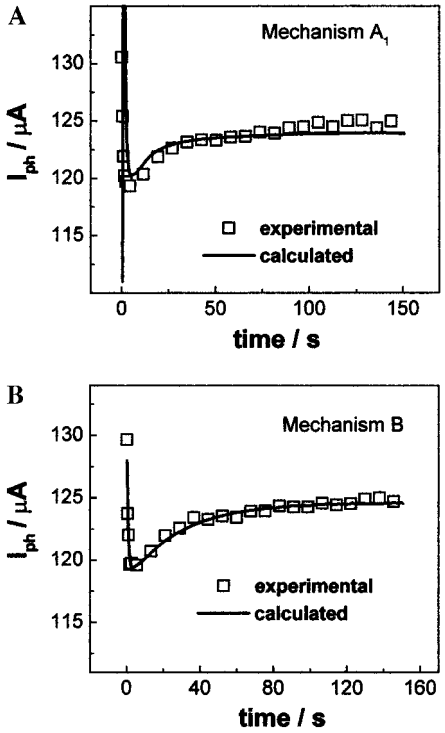

Figure 6. Calculated photocurrent transients at 0.6 V according to mechanism A (a) and mechanism B (b). Model calculations are compared with the experimental data shown in Figure 4.

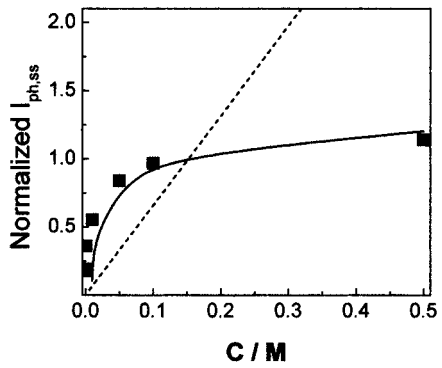

Figure 7. Comparison of the concentration dependence of the steady-state photocurrent with model predictions: (− − −) mechanism A and (—) mechanism B; experimental data (■) in 0.2 M $NaClO_4$ at pH = 3 with photocurrents normalized to the value at 0.16 M.

predict markedly different $I_{ph,ss}$ vs C profiles (Figure 7). The dependence of the steady-state photocurrent with methanol concentration definitively rules out mechanism A. The result of these numeric calculations indicates that the photo-electro-oxidation of short-chain aliphatic alcohols is mediated by $-OH^\bullet$ radicals, or, at least, that this is the main path. In fact, when the constraint $\upsilon_2 = 0$ is released (i.e., reactions 4 and 5 take place in parallel), the fitting does not really improve and additional parameters are required.

Micic et al.,[41] based on their EPR results that, in agreement with Figure 5, denote the very low steady-state concentration of $-OH^\bullet$, favor, on the other hand, the hypothesis of direct hole transfer to methanol. These experimental observations are indeed accounted for by either step 4 or step 5, but they are silent about the nature of the actual reaction mechanism. Heterogeneous photooxidation reactions mediated by $-OH^\bullet$ radicals are not rare;

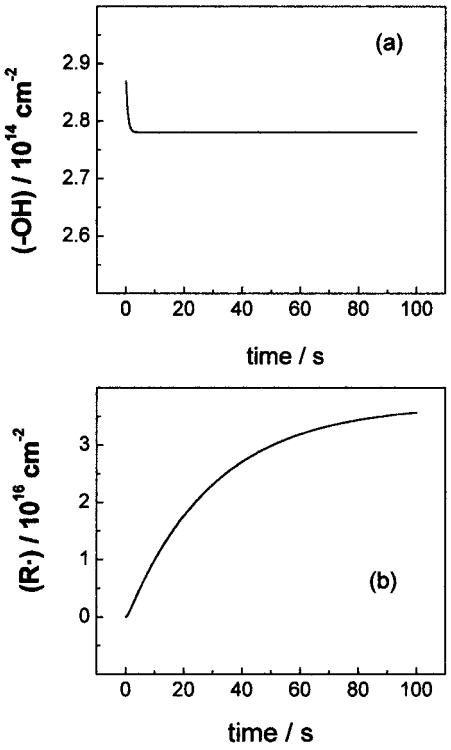

Figure 8. Dependence of the species concentration during the transient at 0.6 V according to mechanism B: (a) −OH concentration and (b) $^{\bullet}CH_2OH$ concentration.

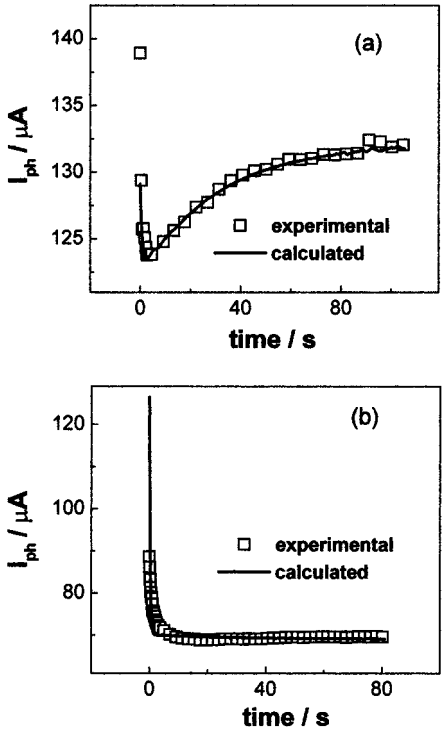

Figure 9. Calculated photocurrent transients at 1.0 V (a) and at −0.3 V (b) according to mechanism B; experimental data (■) taken from Figure 4.

rather, they are the rule.[15−20] However, as already pointed out, the relative contributions of the direct and the $-OH^{\bullet}$ pathways depend essentially on the characteristics of the adsorption of the hole-acceptors.[31] Curves such as that shown in Figure 7 (curve b; see also Figure 2) are common[37] and could, in principle, be interpreted as reflecting Langmuirian methanol chemisorption.[42] The dependence of $I_{ph,ss}$ with methanol concentration cannot be traced back to surface saturation by methanol; not a single feature that could reveal methanol chemisorption on TiO_2 has been detected by ATR−FTIR.[29] Instead, the leveling off of the steady-state photocurrent at the higher methanol concentrations results from the competition between surface recombination (step 3) and the scavenging of $-OH^{\bullet}$ by methanol (step 4). It is well-known that Langmuir−Hinshelwood kinetics does not necessarily imply substrate adsorption.[4]

The proposed mechanism traces the minima observed in the photocurrent transients to the behavior of reactions 2 and 6, the latter being responsible for the increase in photocurrent at the longer times. This can be illustrated using Figure 8, which shows the changes of (OH) and ($^{\bullet}CH_2OH$) during a typical transient; note that the concentration of holes (not shown) attains its steady state value almost immediately. From this figure, it can be seen that the initial photocurrent decay is due to the decreasing number of available hole traps, which rapidly reaches the steady state; obviously, the drop of (OH) is modulated by steps 3 and 4. At the same time, ($^{\bullet}CH_2OH$) increases and the contribution due to step 6 gains in importance. The minimum results because the times scales at which (OH) and ($^{\bullet}CH_2$-OH) reach their steady states differ. Note that in the case of highly reactive radicals, no minimum would be realized and the photocurrent would only decay toward its steady state value. Clearly, the minimum would not be realized either in the case of inert radicals. In agreement, the minimum is barely observable in *tert*-butyl alcohol solutions (Figure 3), as expected from the inability of $(CH_3)_3CO^{\bullet}$ to inject electrons into the conduction band.

Figure 8a also shows that the steady-state surface density of $-OH^{\bullet}$ radicals is about 2 orders of magnitude lower than $(OH)_0$, in line with the experimental results presented in Figure 5. This indicates that the availability of surface hole traps is not a limiting factor in the photo-electro-oxidation of alcohols in aqueous media. In fact, photocurrents are determined by the intrinsic reactivities of the alcohols and their oxidized radicals, i.e., by the respective k_4:k_3 and k_6:k_7 ratios; note that while k_3 should be independent of the nature of the alcohol, k_7 is expected to depend on the electron affinity of $R^{\bullet}$. However, for any guess of a trend for this parameter, one must also include parameters for diffusion to and from the surface.

Figure 9 shows that the proposed mechanism also describes the transients at potential values other than 0.6 V, with the sole assumption that only the recombination constants k_3 and k_7 depend on the applied voltage; incidentally, attempts to include possible potential dependencies of other rate constants did not lead to significant improvements. The potential dependence of k_3 and k_7 is shown in Figure 10. The preexponential factor of k_3 is 3 orders of magnitude larger than that of k_7, as expected from the differences of the reactant distances involved in these interfacial electron-transfer steps. On the other hand, for both k_3 and k_7, $(e/kT)/\{d(\ln I)/dE\} = 3.1 \pm 0.3$, in good agreement with our previous determination of m (cf. inset in Figure 5).

The values of the adjustable parameters that describe the photo-electro-oxidation of methanol according to mechanism B are presented in Table 1. The calculated apparent density of surface hydroxide groups, $(OH)_0 = 2.8 \times 10^{16}$ cm^{-2}, is about 1 order of magnitude higher than that estimated for a perfectly cleaved (001) anatase surface[43] and than that reported for rutile single-crystal electrodes.[35] Since the obtained value refers to the geometric area of the film electrode, this difference should reflect the much higher area exposed by the nanoparticulated TiO_2 films. The rate coefficient for step 1 is, as expected,

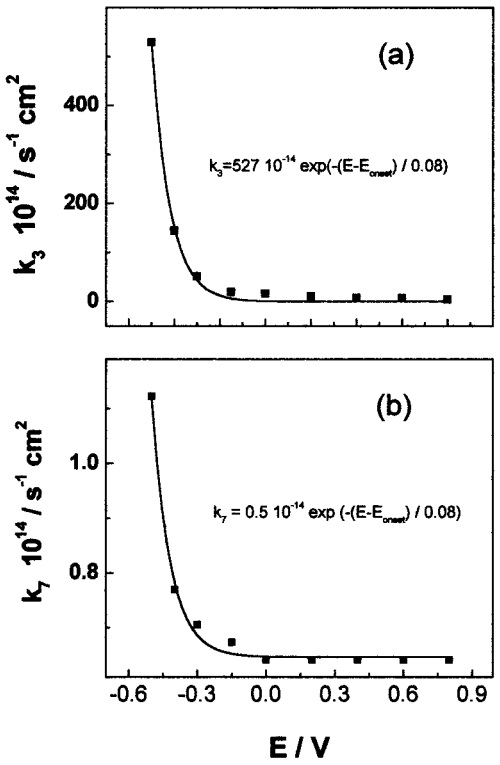

Figure 10. Potential dependence of the rate constants k_3 (a) and k_7 (b). Filled squares are the values obtained according to mechanism B; curves are exponential fits (see text). The E_{onset} value is −0.5 V vs SCE in both cases.

TABLE 1: Model Parameters for Mechanism B ($v_5 = 0$)[a]

$(OH)_0/cm^{-2}$	2.8×10^{16}
$k_1/s^{-1}cm^{-2}$	1.4×10^{15}
$k_2/s^{-1}cm^2$	1.2×10^{-13}
$k_3/s^{-1}cm^2$	4.4×10^{-13}
$k_4(R)/s^{-1}$	1.4
k_6/s^{-1}	1.8×10^{-2}
$k_7/s^{-1}cm^2$	3.8×10^{-14}

[a] Geometric electrode area = 0.6 cm^2; electrode potential = 0.6 V.

considerably lower than the incident flux: most of the incident light is transmitted throughout the film. Moreover, the high density of defects and grain boundaries present in the film act as efficient recombination centers.

The rate constant for hole trapping (eq 2) is ca. 1 order of magnitude lower than that reported by Salvador et al.[35] ($k_2 = 1.2-3.7 \times 10^{-12}$ cm^2 s^{-1}) for rutile single crystal electrodes immersed in 0.1 M KOH (cf. Table 1). Although the films differ appreciably in crystal structure and doping, the different k_2 values should also arise from the markedly different pH ranges that were explored.

k_4, the rate constant for the reaction between OH$^\bullet$ and methanol, can be calculated from the value of the pseudo-first-order constant $k_4(R)$ (Table 1). Assuming that the surface excess of methanol is zero (in the Gibbs convention), k_4 is on the order of 10^{-14} cm^2 s^{-1} for any reasonable guess of the reaction volume. This value is equivalent to a second-order homogeneous rate constant of 10^8 M^{-1} s^{-1}, which is similar to the values reported for the equivalent homogeneous reaction and for that taking place in TiO_2 aqueous suspensions.[21,44] The rate coefficients for step 4 for 2-propanol and *tert*-butyl alcohol are also in the range $k_4(R) = 1.5$ s^{-1}. The lack of sensitivity of this rate coefficient toward the different alcohols is also found for the equivalent homogeneous reactions.[45] Thus, the lower steady-state photocurrents found for 2-propanol and *tert*-butyl alcohol are solely due to the lesser contribution of electron injection into the conduction band (eq 6).

It has been pointed out to us[46] that TiO_2 film electrodes are porous enough to allow for the fast equilibration of methanol within the whole film pore volume. A more accurate description of the rate processes would therefore be much more complex. Yet, the simple approximation of a flat interface allows us to offer a complete description of the processes that take place at the surface of TiO_2 thin film electrodes and conduct to the photoelectro-oxidation of dissolved alcohols.

Conclusions

Photocurrent transients provide a valuable method for assessing the pathways through which the heterogeneous mineralization of dissolved hole acceptors occurs. The shape of the transients is related to the different time scales at which −OH$^\bullet$ radicals are formed and the ensuing interfacial charge-transfer reactions take place. The high initial transient photocurrents are due to the trapping of holes by surface −OH groups. Its fast decay is determined by the recombination of −OH$^\bullet$ with conduction band electrons (step 3), current doubling (eq 6) accounting for the subsequent increase after the minimum. Charge transfer from −OH$^\bullet$ to interfacial R (which is not chemisorbed) is favored by the advanced experimental evidence. Noteworthy, only the recombination processes (eqs 3 and 7) are potential dependent; the values of k_3 and k_7 increase as the applied potential approaches the flat band condition.

Acknowledgment. This work was supported by UBA (grants UBACYT Ex-022, Ex-028, MA-09/93), by CNEA, and by CONICET, (PIP-6634), A.E.R., M.A.B., and S.A.B. are members of CONICET.

References and Notes

(1) Kamat, P. V. *Prog. Inorg. Chem.* **1997**, *44*.
(2) Braun, A. M.; Oliveros, E. *Chem. Rev.* **1993**, *93*, 671.
(3) Kesselman, J. M.; Shreve, G. A.; Hoffmann, M. R.; Lewis, N. S. *J. Phys. Chem.* **1994**, *98*, 8, 13385.
(4) Bahnemann, D.; Pichat, P.; Pelizzetti, E.; Cunningham, J. *In Aquatic and Surface Photochemistry*, Helz, G., Zepp, R., Crosby, D., Eds.; CRC Press: Boca Raton, FL, 1994.
(5) Cunningham, J.; Sedlák, P. *J. Photochem. and Photobiol. A: Chem.* **1994**, *77*, 255.
(6) Ollis D. F.; Al Akabi, H. Eds., *Photocatalytic Purification and Treatment of Water and Air*; Elsevier: Amstertdam, The Netherlands, 1993.
(7) Theurich, J.; Bahnemann, D.; Vogel, R.; Ehamed, F. E.; Alhakimi, G.; Rajab, I. *Res. Chem. Intermed.* **1997**, *23*, 247.
(8) Kormann, C.; Bahnemann D.; Hoffmann, M. R. *Environ. Sci. Technol.* **1994** *25*, 494.
(9) Matthews, R. *J. Phys. Chem.* **1987**, *91*, 3328.
(10) Kim, D. H.; Anderson, M. A. *Envirom. Sci. Technol.* **1994**, *28*, 479.
(11) Vinodgopal, K.; Stafford, U.; Gray K. A.; Kamat, P. V. *J. Phys Chem.* **1994**, *98*, 6797.
(12) Vinodgopal, K.; Bedja I.; Kamat, P. V. *Chem. Mater.* **1996**, *8*, 2180.
(13) Hidaka, H.; Asai, Y.; Zhao, J.; Nohara, K.; Pelizzeti E.; Serpone, N. *J. Phys Chem.* **1995**, *99*, 8244.
(14) Hagfeldt, A.; Lindström, H.; Södergren A.; Lindquist, S. E. *J. Electroanal. Chem.* **1995**, *381*, 39.
(15) Blake, D. M.; Webb, J.; Turchi, C.; Magrini, K. *Solar Energy Mater.* **1991** , 24, 584.
(16) Tunesi, S.; Anderson, M. *J. Phys. Chem.* **1991**, *95*, 3399.
(17) Kesselman, J. M.; Weres, O.; Lewis, N. S. Hoffmann M. R. *J. Phys. Chem. B* **1997**, *101*, 2637.
(18) Gerisher, H.; Heller, A. *J. Phys. Chem. B* **1991**, *95*, 5261.
(19) Brezová, V.; Staško, A.; Biskupic, S.; Blazková, A.; Havlínová B. *J. Phys. Chem.* **1994**, *98*, 8977.
(20) (a) Peterson, M. W.; Turner, J. A.; Nozik, A. J. *J. Phys. Chem.* **1991**, *95*, 221. (b) Shaw, K.; Christensen, P.; Hamnett, A. *Electrochem. Acta* **1996**, 41, 719.
(21) Mao, Y.; Schöneich C.; Asmus, K. D. *J. Phys. Chem.* **1991**, *95*, 10080.

(22) Aas, N.; Pringle, T. J.; Bowker, M. *J. Chem. Faraday Trans.* **1994**, 90, 1015.
(23) Kim, K. S.; Barteau, M. A. *Surf. Sci.* **1989**, *223*, 13.
(24) Brinkley, D.; Engel, T. *J. Phys Chem.* **1998**, *102*, 7596.
(25) Kaise, M.; Nagai, H.; Tokuhashi, K.; Kondo, S.; Nimura, S.; Kikuchi, O. *Langmuir* **1994**, *10*, 1345.
(26) Marcì, G.; Sclafani, A.; Augugliaro, V.; Palmisano, L.; Schiavello, M. *J. of Photochem. and Photobiol. A: Chem.* **1995**, *89*, 69.
(27) Lepore, G. P.; Vlcek, A. Langford, C. H. *Photocatalytic Purification and Treatment of Water and Air*; Ollis, D. F., Al Akabi, H., Eds., Elsevier: Amstertdam, The Netherlands, 1993; p 95.
(28) Gamble, L.; Jung, L.S.; Campbell, C.T. *Surf. Sci.* **1996**, *348*, 1.
(29) Mandelbaum, P. A.; Bilmes, S. A.; Weisz, A. D.; Regazzoni A. E.; Blesa M. A. 12th International Conference on Photochemical Conversion and Storage of Solar Energy, Berlin, Germany, August 9−14, 1998.
(30) Rodríguez, R.; Blesa M. A.; Regazzoni, A. E. *J. Colloid Interface Sci*. **1996**, *177*, 122.
(31) Regazzoni, A. E.; Mandelbaum, P. A.; Matsuyoshi, M.; Schiller, S.; Bilmes, S. A.; Blesa, M. A. *Lagmuir* **1998**, *14*, 868.
(32) Bohem H. P. *Disc. Faraday Soc*. **1971**, *52*, 264.
(33) Mandelbaum, P. A.; Bilmes, S. A.; Regazzoni A. E.; Blesa, M. A. *Solar Energy* **1999**, *65*, 75.
(34) Candal, R. J.; Zeltner, W. A.; Anderson, M. A. *J. Adv. Oxid. Technol.* **1998**, *3*, 270.
(35) Salvador, P.; García González M. L.; Muñoz, F. J. *J. Phys. Chem*. **1992**, *96*, 10349.
(36) Rothenberger, G.; Moser, J.; Greatzel, M.; Serpone, N.; Sharma, D. K. *J. Am. Chem. Soc.* **1985**, *107*, 8054.
(37) Nogami G.; Kennedy, J. H. *J. Electrochem. Soc*. **1989**, *136*, 2583.
(38) Schoenmakers, G. H.; Vanmaekelbergh, D.; Kelly, J. J. *J. Chem. Soc., Faraday Trans.* **1997**, *93*, 1127. (b) Hykaway, N.; Sears, W. M.; Morisaki H.; Morrison, S. R. *J. Phys. Chem*. **1986**, *90*, 6663.
(39) Dutoit, E. C.; Cardon F.; Gomes W. P. *Ber. Bunsen-Ges. Phys. Chem*. **1975**, *79*, 1206.
(40) Bolton, J. In *Aquatic and Surface Photochemistry*; Helz, G., Zepp, R., Crosby, D., Eds.; CRC Press: Boca Raton, FL, 1994.
(41) Micic, O. I.; Zhang, Y.; Cromack, K. R.; Trifunac A. D.; Thurauner, M. C. *J. Phys. Chem* **1993**, *97*, 13284.
(42) Wahl, A.; Ulmann, M.; Carroy, A.; Jermann, B.; Dolata, M.; Kedzierzawski, P.; Chatelain, C.; Monnier, A.; Agustinski, J. *J. Electroanal. Chem* **1995**, *396***,** 41.
(43) Bohem, P. H.; Herrmann M. Z. *Anorg Chem*. **1967**, *352*, 156.
(44) Matthews, R *J. Chem. Soc., Faraday Trans.* **1984**,*80*, 457.
(45) Motohashi, N.; Saito, Y. *Chem. Pharm. Bull.* **1993**, *41*, 1842.
(46) M. Anderson, private communication.